A G9A/GLP INHIBITOR INCREASES EXPRESSION OF SELP(P-SELECTIN) IN A CELL LINE AND HSCS

SOHEILA JALALI

MSc. Biomolecular Sciences

Research Project 2018/2019

S3613151

Supervisor: Daozheng Yang

Examiner: Prof. Dr. Gerald de Haan

Abstract

Selp (P-selectin) gene expression has been found to be highly upregulated in ageing hematopoietic stem cell (HSC) populations. Although some evidence linking epigenetic enzymes to age-related differential expression exists, few papers focus on finding a link between these and Selp. In this project, we found that inhibition of the H3K9 mono- and di-methyltransferase enzymes G9a and GLP using UNC0638, increases the expression of Selp RNA and protein levels in a cell line and Lin-/Sca+/cKit+ (LSK) cells isolated from young mice. We determined that the time-frame in which effects of the inhibitor are best observed is 1-2 days in both cell types. We further saw that increased Selp levels accompanied an increased self-renewal phenotype in the primary cells. Finally we found that P-selectin expression levels did not play a deterministic role in the colony-forming potential of aged long term HSCs in-vitro. Connecting the findings to literature, we suggest a potential link between Selp, senescence and the SASP. Further investigations may hold promise for translational applications.

TABLE OF CONTENTS

INTRODUCTION

The ageing process affects almost every cell type, tissue system and organism, manifesting in the form of gradual functional decline and eventual mortality. Understanding the molecular mechanisms underlying ageing has become one of the primary focuses of biomedical research. Indeed, decoupling the causes from the consequences of ageing is essential to future development of anti-ageing, anti-cancer and rejuvenation therapeutics. In this regard, adult stem cells, especially those of the hematopoietic system, hold great promise for current and future therapeutic solutions.

Hematopoietic stem cells (HSCs) are responsible for giving rise to every type of mature blood cell throughout the lifespan of mammals. These multipotent stem cells primarily reside in the bone marrow (BM) niche and are organized hierarchically in their ability to differentiate into the various blood cell lineages [1]. A relatively low number of quiescent HSCs act as a sort of rejuvenation reservoir with the ability to replace all circulating blood cells. However, they too have been shown to undergo ageing with loss of function and other characteristic phenotypes emerging over time. In fact, several publications have highlighted (epi)genetic changes comprised of upregulation and downregulation of distinct genes with age [2,3]. The established phenotypes accompanying ageing within the HSC compartment include increased stem cell number, reduced (lymphoid) differentiation potential and a skew toward the myeloid and platelet lineages [4,5,13]. Their functional decline with age has also been referred to as senescence [6] with modelling studies revealing that replicative senescence could explain the increased number of cells with lowered functionality [7].

The influence of cell-extrinsic and intrinsic factors on the ageing phenotypes remains somewhat ambiguous [8] but there is unarguably a complex interplay between multiple "hallmarks of ageing" [9]. A meta-data analysis carried out by the "Ageing biology and stem cells" group at the European Research Institute for the Biology of Ageing (ERIBA) assesses the congruity of the transcriptional upregulation and downregulation profiles of aged HSCs across several studies. Using and internally developed gene set enrichment analysis (GSEA) protocol, a set of "signature" genes was found which were consistently reported across most publications to be either up- or down-regulated with age. The genes were ranked by the number of times they were reported and the extent to which they were differentially expressed in aged HSCs. Interestingly, several of the top "hits" in this list of ageing genes happened to be involved with cellular adhesion and signalling, putting them at the interface between extrinsic and intrinsic factors.

The top "hit" through this assessment was the **Selp** gene which was not only the most consistently reported differentially expressed gene in majority of the analysed papers, but also one of the most highly upregulated (Renders, S. et. al. submitted, 2019). Selp encodes the P(latelet)-selectin protein (also known as CD62P) which is an adhesion molecule whose role has been largely characterized in the context of the circulatory system where it is expressed on the surface of platelets and endothelial cells that become activated by certain inflammatory signals. Generally, this is localized at the site of injury or at the site of infection where it is required that aggregation and cell-cell interactions can occur. P-selectin glycoprotein ligand 1 (PSGL1) is a ligand that binds to P-selectin and is expressed on the surface of leukocytes that can then interact with platelets and endothelial cells and form mixed cell aggregates [10]. Not much has been characterized in relation to P-selectin's role within the HSC niche. However, it was reported that $Selp^{-/-}$ cells were more efficient at repopulating the bone marrow than wild type counterparts [11].

Several studies done on HSCs have reported Selp upregulation as a result of various investigations associated with inflammatory cytokines and epigenetic perturbations. Since P-selectin is known to be expressed in platelets, it is not surprising that one such report describes its upregulation in the context of megakaryopoiesis. Haas *et al.*, 2015 [12] found that upon induction of inflammation by administration of pI:C or LPS, Selp was upregulated with a number of other megakaryocytic genes in HSCs. The authors, and others [13] refer to P-selectin as a "megakaryocytic protein" and show that a

protein level increase occurs post-transcriptionally. Although this alludes to a potential effect of inflammation, in order to follow up on the "ageing signature" findings of the de Haan lab, we turned our focus toward potential epigenetic regulators of Selp.

A repertoire of epigenetic marks play a role in the mediation of gene expression. These may be present either directly on the DNA or associated with specific amino acid residues of histone proteins. Each type of mark can affect gene expression by altering chromatin structure and/or accessibility to the promoter. While DNA methylation is primarily associated with gene silencing, there are a variety of histone marks (methylation, acetylation) that can either cause upregulation or downregulation of genes depending on where they are found [13]. With age, there are several histone marks that are reported to be dysregulated along with the enzymes that mediate them. For instance, López-Otín et. al. [9] reported that there is a global reduction in H3K9 methylation (repressive mark) with age. Changes in the amount and patterns of H3K27 and H3K4 methylation have also been characterised with ageing along with enzymes such as Dnmt1,3a and 3b [2].

There are multiple instances in which Selp expression was altered when H3K9 methyltransferases were manipulated. In a 2016 paper, Djeghloul et. al. [14] found that a $SUV39h1^{null}$ mice had an increased expression of Selp in their HSCs compared to wild type. They found that overall H3K9me3 levels were reduced in old HSCs of humans and mice. Use of Chaetocin, an inhibitor of SUV39h1 on $Lineage^{-}/Sca^{+}/cKit^{+}$ (LSK) cells also showed that B cell potential was decreased while myeloid potential was unaffected. They were able to induce the age-associated phenotype of B-cell potential loss by knocking down SUV39h1 and rescue the B-cell potential in aged mice by overexpression of this H3K9me3 methyl transferase.

Another pair of epigenetic enzymes, also involved in H3K9 methylation, have been reported to play roles in hematopoietic stem cell differentiation [21] and DNA damage associated senescence [18]. G9a(EHMT2) and G9a-like protein (GLP/EHMT1) are known to mono- and di-methylate lysine 9 (and 27) on histone H3 to facilitate silencing of genes, mainly during differentiation. In this regard, they have also been shown to function in concert with the PRC2 complex [15]. The two enzymes are said to interact and form a heteromeric complex [16, 17] with both possessing a catalytic SET domain by which they bind the lysine on histone 3. Their degradation with age has also been linked to the induction of the senescence associated secretory phenotype (SASP) cytokines IL-6 and IL8 [18].

In their paper, Ugarte *et al.*, 2015 [19] investigate the effect of a G9a/GLP specific inhibitor UNC0638 which is known to act as a competitive substrate, binding to the SET domain of the enzymes [20]. According to their findings in mouse and others on human HSCs [21], treatment with this inhibitor enhances HSCs' self-renewal, with decreased differentiation in vitro. As a supplementary finding, they report a two-fold increase in Selp expression upon treatment with this inhibitor. Relatedly, another study [22] showed that H3K9me2 demethyltransferase $JMJD1B^{-/-}$ led to downregulation of Selp further suggesting that H3K9me2 methylation is involved in Selp regulation.

Thus, the aim of this project was to investigate whether the inhibition of G9a/GLP can increase Selp expression on the RNA and protein levels and if so, what implications this may have in understanding the age-related increase in the transcription of Selp. The use of UNC0638 has been well documented and its specificity for G9a/GLP proven [20]. The approach was to test the inhibitor by varying the concentrations and exposure times in a Selp expressing cell line and then in primary HSCs isolated from young mice (low Selp expression). In addition, some experiments in aged HSCs were conducted to investigate functional effects of P-selectin in old HSCs.

MATERIALS AND METHODS

Cell line culture

Although most experiments were conducted C2C12 mouse myoblastic adherent cells, 32Ds and NIH/3T3 were also cultured for initial experiments. For C2C12 and 3T3 culture, cells were maintained in T75 flasks with 10 ml of Dulbecco's Modified Eagle Medium (DMEM) with 10% HiFCS and 1% PenStrep. Cells were incubated at 37°C and passaged 1:10 every alternate day or when confluency of 70%-80% was observed. For passaging, first PBS was used to wash the cells, then either Trypsin or Accutase (Stem Cell Technologies) was added in the amount recommended by the manufacturer. When using Trypsin, cells were incubated with the enzyme for 5 minutes at 37°C before adding medium to stop the reaction. When using Accutase, cells were left at room temperature for 7-10 minutes. In both cases detachment was confirmed under the microscope. Initial dose titration experiments were conducted using Trypsin while Accutase was used in the time-frame studies.

32Ds were maintained in RPMI medium supplemented with 10% HiFCS and 1% IL-3. These cells were maintained in a T25 flasks, incubated at 37°C and passaged 1:10 every alternate day.

Inhibitor treatments

C2C12 cells at passage number 6-10 were used in all experiments. For inhibitor treatments, cells were seeded at 40,000 cells per well in a 6 well plate with 2 ml of medium per well. UNC0638 was prepared at concentrations 0.125, 0.25, 0.5, 1.0, 2.0 and 4.0 uM by serial dilution of the inhibitor in medium and DMSO-medium mix to maintain the concentration of DMSO across treatments. Each plate contained an untreated control (NC), a DMSO control and 3 inhibitor treated wells. Thus, two plates were set up simultaneously to cover six treatment concentrations. Cells were harvested after 3 days. This experiment was repeated four times.

For time-frame experiments C2C12 cells were seeded at 150,000 for 1-day, 100,000 for 2-day and 50,000 for 3-day analyses. Here, only 1 uM concentrations were used and were prepared by directly pipetting 2ul of the drug or DMSO (for control) into the 2ml medium. Cells were harvested at Day 1, 2 and 3. This was repeated two times.

Preparation of the treatment dilution series for young mouse LSK cells was done in a similar way to that described for C2C12s. Volumes for adjusted for 200ul total well volume as per 96-well plates. The range was adjusted to only include four concentrations 0.25, 0.5, 1.0 and 2.0 uM. These cells were harvested at 1- and 2-day time-points.

Cell harvesting

Adherent cell lines were harvested by first discarding the medium washing the wells with PBS and then adding Accutase/Trypsin as described above. For 6-well plates, 200ul of enzymes per well was sufficient to detach cells. Resuspension by addition of 800 ul medium and repetitive pipetting (5-10 times) resulted in single cell suspensions. Cells were mixed Trypan blue in a 1:1 ratio and counted by loading onto a haemocytometer. Cell concentrations were calculated, and appropriate volumes of cells were then taken for RNA and protein analyses.

RNA extraction

For RNA extraction from cell lines (C2C12) approximately 500,000 cells were harvested. In cases where this number was not obtainable, a minimum of 200,000 was necessary to obtain RNA of reasonable quality. Cells were washed with PBS + 0.2% BSA and then resuspended in 350ul of RNeasy RLT Plus lysis buffer. Homogenisation was carried out using a 25G needle and syringe. The homogenate was then stored at -80°C until required for RNA extraction. Prior to extraction the homogenate was thawed in a 37°C water bath or at room temperature. RNA was extracted in accordance with the RNeasy Plus Mini kit from Qiagen in a low copy room. RNA was quantified using a Nanodrop machine.

In case of primary cells, 100 ul (approximately 10,000-15,000) of cells were harvested by resuspending the cells in the medium. Lysis was carried out in accordance with the Nucleospin® RNA XS RNA isolation kit manufactured by Macherey-Nagel.

cDNA preparation

For preparation of cDNA, in most cases, RNA volumes were calculated corresponding to 1ug and first incubated with 1ul oligo DT and 10 mM dNTP mix with the mixture topped up to 12ul using PCR-grade water. In cases where 1ug could not be obtained from all samples, the lowest obtainable amount was used across samples. The mixture was heated to 65°C for 5 minutes followed by quick chill on ice. A mixture of 5X first strand buffer, 0.1M DTT and RNaseOUT™ Recombinant Ribonuclease Inhibitor was prepared in the ratio 4:2:1 and 7ul added to the original mix. This was then incubated at 37°C for 2 minutes. Finally, 200 units (1 ul) of M-MLV RT enzyme was added to each tube and the 20ul mixtures incubated at 37°C for 50 minutes followed by inactivation at 70°C for 15 minutes. The cDNA was either stored at -20°C or used directly for qPCR.

qPCR

All qPCR experiments were set up such that the columns represented the gene of interest with rows representing different samples. Every sample was pipetted in triplicate. Thus, the cDNA was diluted such that the final volume would allow for 2.5ul of sample per well across three replicates and generally, four genes i.e. HPRT, G9a, GLP and Selp. The primer mixes were prepared such that 7.5 ul of the mix could be pipetted into each sample for that gene block.

The table represents the volumes for a single well and these were adjusted as per required volumes.

2 x SYBR green mix	5 ul
PCR grade Water	2.45 ul
Forward primer	0.025 ul
Reverse primer	0.025 ul

After pipetting (10ul reaction volume), the PCR plate was spun down briefly and then placed in the LightCycler® 480 and run under an amplification programme of 40 cycles.

FACS Analysis

FACS analysis of treated C2C12s and young mouse LSKs was conducted on the BD FACSCanto II device. For cell line sample analysis, PI and blank controls were used and 0.5ul of Selp antibody conjugated to BV605 was added to 100ul of cells. For analysis of primary cells, single stain controls were prepared in

Incubation with respective amounts of antibody was carried out for 30 mins at 4°C followed by washing with PBS + 0.2% BSA and the addition of PI to samples, PI control and single-stain controls (except PE).

Intracellular FACS

100ul of cells from various treatment conditions were aliquoted in individual FACS tubes along with tubes for blank and secondary antibody only controls. 500ul of BD fix/permeabilization buffer was added to cells and tubes were left to incubate for 15 minutes at 4°C. A 1x dilution of the 10x BD Perm/Wash™ buffer was prepared and cells were then washed twice with this solution by centrifuging at 500G for 5 minutes. For blocking, 300ul of of 4% BSA in 1x BD Perm/Wash™ buffer was added to cells and left for 30 minute incubation at 4°C. Tubes were spun down and supernatant discarded with cells resuspended in the left over liquid. Fresh tubes were taken into which 50ul of cell suspension was added.

Rabbit anti-mouse, polyclonal anti-H3K9me2 antibody (Active Motif catalogue number 39239) was used as the primary antibody and prepared in a 1:500 dilution. 50ul was added to 50ul of cells for 60 minute incubation at 4°C. Two subsequent washes were performed in 1x BD Perm/Wash™ buffer and then secondary antibody (1:500 dilution) was added again, in equal volumes so as to prevent further dilution of the antibody. This too was incubated as above and washed twice before analysis on the BD FACS Canto II machine.

FACS sorting

Stemspan medium was prepared with the addition of HiFCS and murine cytokines Flt3, SCF and IL-ll and pipetted into wells of round-bottom 96-well plates. Hematopoietic stem cells were obtained by harvesting hip, legs, sternum and spine from young (4 month old) c57/black 6 mice for treatment with UNC0638, and old (24-27 month) mice for functional studies of $Selp^{high}$ and $Selp^{low}$ cells. Bones were cleaned and crushed in accordance with the standard laboratory protocols and cell numbers determined using the Medonic cytometer.

Preparation of staining mixtures was done in accordance with the table below. Approximately 5000-10000 of $Lineage^{-}/Sca^{+}/cKit^{+}$ (LSK) cells were sorted per well from young mice for inhibitor treatments. This was dependent on number of available cells. In case of old mice, LSK, $CD150^{+}$ and $CD48^{-}$ (SLAM) were stained with the addition of P-selectin antibody. In this case the cKit and CD150

fluorophores were altered to as to accommodate Selp-PE. For single cell colony assays, a single long term (LT) HSC was sorted per well from a $Selp^{high}$ (gated at highest 30%) population and separately from the $Selp^{low}$ gated populations. Cells were sorted using the Beckman Coulter MoFlo XDP cell sorter.

Surface Marker	**Fluorophore**
Sca1	Pacific blue
cKit	PE/FITC
CD150	PE-Cy7/APC Fire 750
CD48	A647
B220	A700
CD11b	A700
CD3	A700
Gr1	A700
Ter119	A700
P-selectin (CD62P)	PE

Colony Forming Unit – Granulocyte Macrophage (CFU-GM)

Preparation of the Methocult medium was done in accordance with manufacturer protocols (Stem Cell Technologies) with the addition of appropriate cytokines for CFU-GM. 250 $Selp^{high}$ or $Selp^{low}$ cells were sorted directed into 2.5ml of the medium. SCF, Flt3 and IL-11 were added post-sort. Medium was vortexed and poured into 10mm dishes using a needle and syringe. Plates were incubated at 37°C and scored at 7- and 14-day time points.

Data Analysis

Most of the data analysis including linear regressions, t-tests, dose response curves, significance calculations were carried out using Graphpad Prism software (version 7.0). Histogram comparisons from FACS analyses were analysed using FlowJo's in-built "compare populations" tool that provides several comparative metrics including Overton percent positive [26, 27].

RESULTS

DOSE-TITRATION OF UNC0638 ON C2C12 CELLS

C2C12 cell line can be used for investigating changes to Selp levels

A set of preliminary experiments were carried out to determine the constitutive expression of Selp in four cell lines, namely 32D Selp overexpression (OE) and empty vector (psf912) (EV), C2C12 and NIH/3T3. As per information from online databases (Genevisible, BioGPS) it was expected that Selp expression in the adherent cell lines C2C12 and 3T3 would be mid-to-high whereas that of 32D empty vector (as in wild type) would be very low. An initial qPCR was run on all these available cell lines to determine which would be most ideal for investigating perturbations to Selp. The qPCR confirmed that relative to HPRT, C2C12s and NIH/3T3 have a higher expression than the 32D EV (Figure 1), with expression in 3T3s being marginally higher than in C2C12s. Further, a qPCR checking G9a and GLP values in the 3T3 and C2C12 cells showed comparable expression between both cell lines. However, Qiagen's RNeasy Mini handbook mentions that RNA levels in NIH/3T3 cells can be generally low and more cells may be required for RNA extraction. Thus, C2C12s were chosen as the cell line in which to conduct further experiments.

A

Cell Line	C_t Values	
	HPRT	Selp
32D EV	24.73	28.02
32D Selp OE	20.61	13.71
3T3	21.86	22.43
C2C12	22.60	23.64

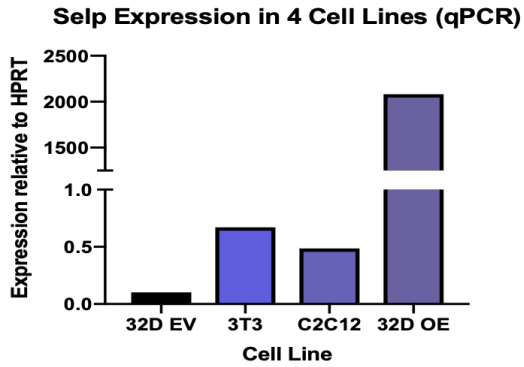

B

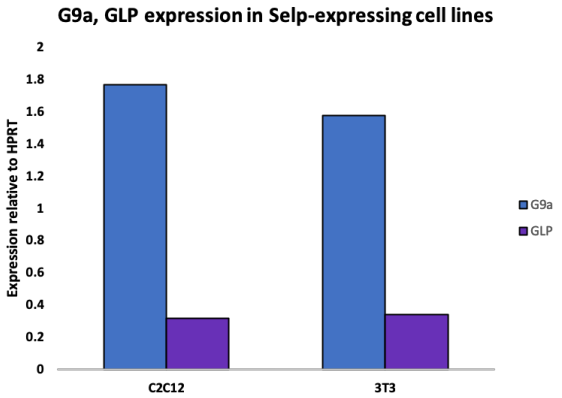

Figure 1: (A)The raw Ct values and plotted expression levels of the four tested cell lines 32D EV, NIH/3T3, C2C12 and 32D Selp Overexpression (B) G9a and GLP expression levels (relative to HPRT) in C2C12 and NIH/3T3 cell lines

C2C12 survival is inhibited at high doses of UNC0638

Since it has been reported that HSC viability decreases at concentrations greater than 1 uM UNC0638 (Ugarte *et al.*, 2015), a range that included this concentration was used to determine the IC50 in C2C12 cells. Thus, the dose titration was done using 0.125, 0.25, 0.5, 1.0, 2.0 and 4.0 uM obtained through serial dilution of the compound in medium with DMSO, maintaining equivalent DMSO concentrations across treatments. Based on the 3-day exposure time, the IC50 was calculated to be 1.284 uM with cell viability appearing to gradually decline between 0.125 and 1.0 uM (Figure 2A). Indeed, at the 3-day time point most cells in wells with higher concentrations of the drug were dead, with only one replicate of the experiment having any live cells in the 4.0 uM concentration. It was for this reason that the qPCR data is limited to concentrations up to 1uM (Figure 2B). However, it was observed that at earlier time points, cells in wells with higher concentrations were still viable although not quantified.

Selp RNA expression in C2C12 cell line increases on treatment with UNC0638 in a non-dose dependent manner

When treated with a range of concentrations, the Selp RNA expression levels in C2C12 cells increased across all concentrations. The average fold change compared to DMSO controls was 1.86 (Figue 2B). A linear regression of RNA fold change across the treatment dosages produced an almost flat line, with insignificant slope (Figure 2B). This led to the conclusion that the expression changes in response to UNC0638 are not dose-dependent at least for the range of concentrations used in these experiments. It also suggested that any one of these concentrations could be selected for further experiments without largely impacting the effect seen on the transcription levels.

Additionally, since there didn't appear to be any dependency on the concentrations used, it was reasonable to group all treatments as a single data set and compare Selp expression to the DMSO group. On average, the expression relative to HPRT in the DMSO group was 0.025 whereas in the treated group it was 0.043 (Figure 2C). Thus, this comparison led to identification of a highly significant increase in UNC0638 treated samples compared to the DMSO controls.

Selp protein expression appears to increase in a dose dependent manner

To follow up on the RNA expression data, FACS analysis of treated C2C12s stained with P-selectin antibody conjugated to BV605 was conducted on one of the replicates. Since FACS analysis is not limited by the cell number, in this case it was possible to obtain protein level data for cells subjected to 2.0 uM treatments as well. The median Selp-BV605 signal for each sample was taken based on a similar number of measured events. The fold change was calculated by normalizing to the median Selp-BV605 value in DMSO. The overall BV605 shift can be visualized in histogram form using the "compare populations" tool on FlowJo. Using this in-built analysis, the Overton percent positive is quantified which is essentially a histogram subtraction. Here, the percent of "positive" events obtained after subtracting the control fluorescence from that of the treated population is calculated as a numerical value [26]. This value was quantified as 8.3, 17.7 and 50.3 for 0.25uM, 1.0uM and 2.0 uM treatments respectively, indicating some dose-dependency. In fact, the significance of the linear regression slope (Figure 2D) is strongly influenced by the highest concentration, where more cells are dead or dying.

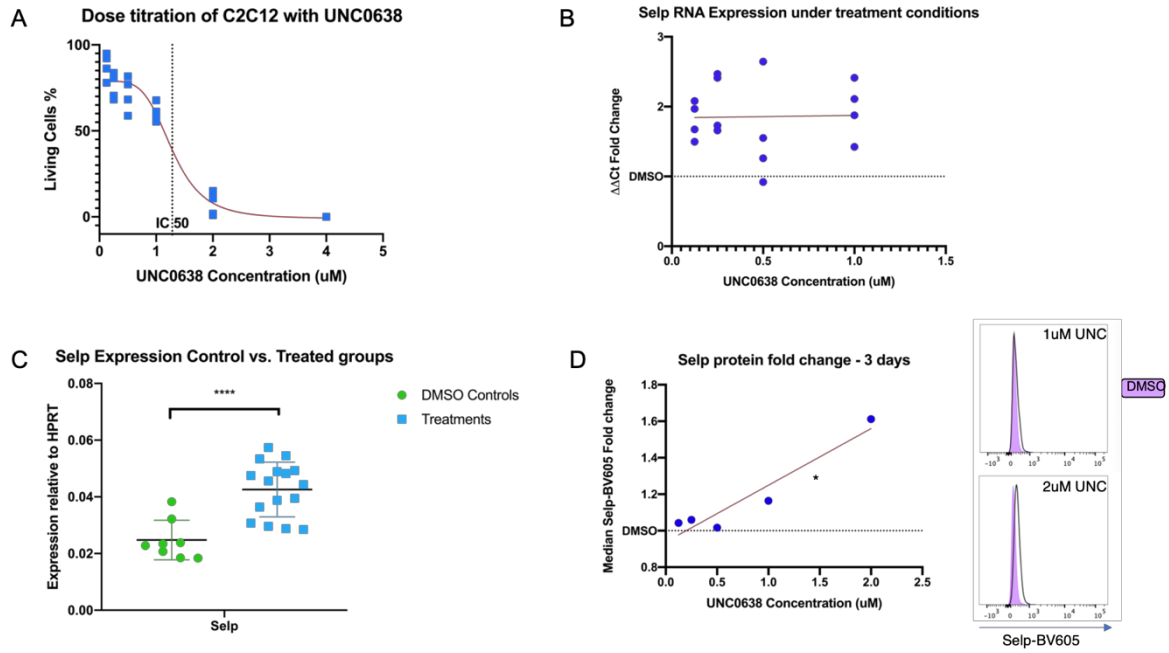

Figure 2: (A) Dose titration effect of UNC0638 on viability of C2C12s in culture for 3 days (B) RNA expression ΔΔCt fold-changes of Selp at titrated doses of inhibitor normalised against DMSO (n = 4) with linear regression line (red) (C) Grouped Selp RNA expression analysis of all treatment conditions versus DMSO control samples D) FACS analysis for membrane-localised P-selectin (n=1) plotted as median fluorescence signal for BV605 against inhibitor dose with corresponding histogram plots of 1uM and 2uM Selp-BV605 shift compared to DMSO (tinted).

SINGLE DOSE TIME-FRAME INVESTIGATION ON C2C12S

After establishing the effect of UNC0638 on Selp expression at a 3-day time point at various concentrations of the drug, it was considered that an earlier time point would be preferable to use for primary cells in culture. If effective, the post-treatment analysis could then be carried out on largely undifferentiated cells. Based on the 3-day results, 1uM was deemed as a suitable concentration at which to obtain observable effects. Thus, C2C12 cultures were set up so as to be harvested and analysed at 1, 2- and 3-day time points.

Effect of UNC0638 treatment on Selp RNA and protein levels

Using separate 6-well plates to incubate cells for each time point, cells were harvested independently each day for RNA and FACS analysis. Data from multiple repeats indicate that the Selp RNA levels are already significantly upregulated on the first day after treatment. Relative to DMSO, there is significantly higher Selp expression in treated samples on the first and third days of treatment (Figure 3A). Indeed, the mean expression fold change between Day 1 (2.88) and Day 3 (2.84) is similarly maintained (Figure 3B) while the actual expression levels of Selp relative to HPRT seem to decrease from Day 1 to Day 3. Unfortunately, RNA data from Day 2 was of poor quality and therefore not used

in the comparative analysis. Yet, the data is sufficient to conclude that exposure time of less than 3 days i.e. 1 to 2 days should be enough to see effects of the inhibitor in stem cells before they have time to differentiate.

Compared to qPCR data, FACS analysis showed a slightly different trend for P-selectin protein levels relative to RNA levels. In this case, Overton percent positive values for BV605 were 15.8, 28.8 and 25.9 for the first, second and third days respectively, meaning that at every time point inhibitor treated cells were more positive for P-selectin expression than DMSO controls (Figure 3C). The effect from transcription to translation seems to be staggered in that RNA levels are relatively higher on Day 1 (earlier) while protein levels are higher on Day 2 and 3.

H3K9 di-methylation is reduced at early time points

Since UNC0638 is an inhibitor of G9a/GLP, it was expected that the addition of the inhibitor would cause a decrease in H3K9me2 levels in the cells. This was tested using intracellular FACS to detect APC-conjugated secondary antibody after first incubating with an antibody against H3K9me2. Once again, a population comparison between DMSO and treated cells on each day was carried out in FlowJo to visualise the shift in the APC positive signal (Figure 3D). The results indicated that for the first two days after treatment, the H3K9me2 levels of the treated cells was lower than that of the DMSO control. However, on the third day, the trend is the opposite. This relates well to the RNA findings wherein Selp RNA expression is reduced by Day 3.

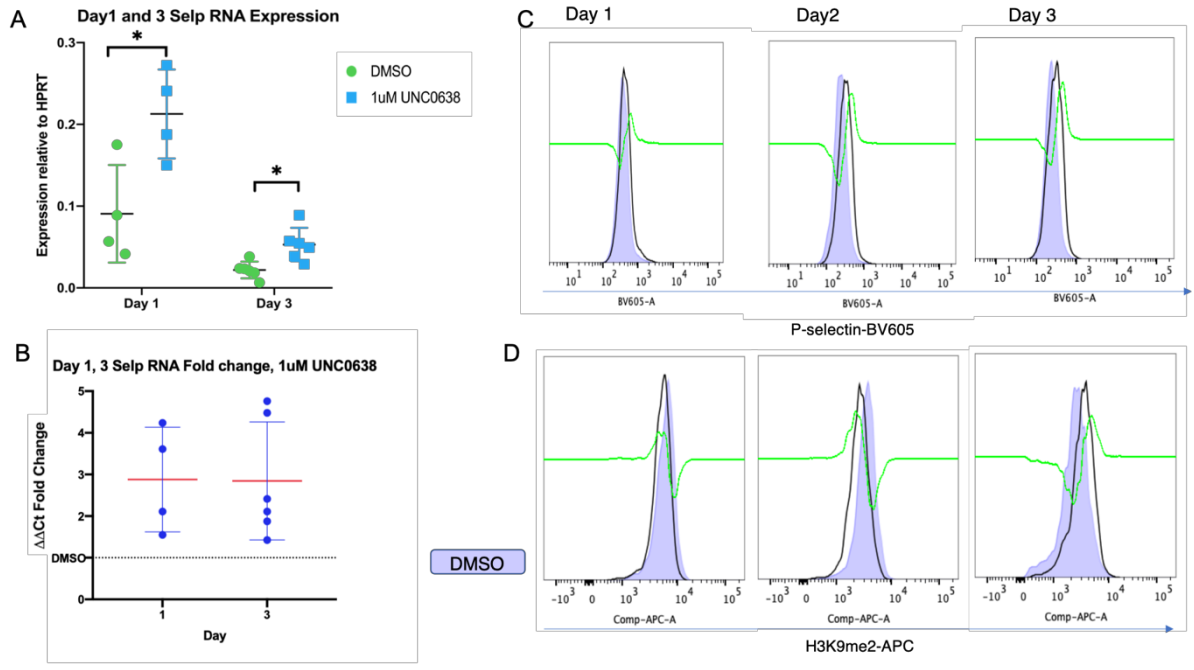

Figure 3: (A) Selp RNA expression levels in treatment (1uM) vs. DMSO controls on Day 1 and 3 (B) Selp RNA expression fold-change under 1uM UNC0638 treatment on Day 1 and Day 3 (C) The P-selectin-BV605 histogram comparison of treated (1uM UNC0638) vs DMSO (tinted) samples at Days 1, 2 and 3. (D) Histogram comparison of H3K9me2-APC signals in treated vs DMSO on Days 1, 2, and 3.

TREATMENT OF YOUNG MOUSE LSK CELLS WITH UNC0638

Dose titration of UNC0638 reveals dose-dependent effect on Selp expression

In the case of young mouse LSKs, dose titration experiment across 1- and 2-day time points could only yield enough cells for FACS analysis. Unfortunately, here too, good quality data could not be obtained for Day 2. However, the data obtained from Day 1 shows increasing P-selectin signal (median Selp-BV605) with increasing concentrations of the inhibitor until 1uM and a slight drop thereafter (Figure 4A). The FACS histograms overlaying the Selp-BV605 signal for DMSO, 0.5uM and 1uM UNC0638 (Figure 4A) confirm that there is a visible shift in the fluorescence signal related to P-selectin expression. At 1uM UNC0638 concentration, the P-selectin protein levels peak.

In order to obtain a more in-depth picture of the effect of the inhibitor on LSKs, the experiment was repeated using only 1uM concentration but on a larger number of cells so as to have enough for RNA and protein level analyses. Here, the RNA fold change and protein fold change appear to increase on Day 2 with a more pronounced effect at the RNA level exhibiting a mean fold change of 1.65 across the 2 days compared to 1.2-fold change on the protein level (Figure 4B). In general, treated cells have a higher Selp expression at RNA and protein levels as compared to DMSO controls.

The percentages of LSK cells is maintained at a higher level (95.1%) in inhibitor-treated cells as compared to DMSO controls (83.6%) (Figure 4C). At increasing doses, there appears to be a linear trend of increasing LSK percentage as concentrations increase. On Day 1 and 2, the slope of the linear regression line across inhibitor concentrations is significant (Figure 4D). Thus, the trend shows that the LSK fraction increases with treatment concentrations. Therefore, the LSK/SLAM Long Term (LT-HSC; $CD150^{+}$, $CD48^{-}$) population was also checked wherein it was found that the percentage of cells within the gate increase at increasing concentrations of the inhibitor (Table 1, Figure S1). However, this pattern was not reproduced when the experiment was repeated with only 1uM concentration of UNC0638. Overall, it was noted that an increase in Selp RNA and protein level is accompanying the self-renewal phenotype when LSKs are exposed to UNC0638.

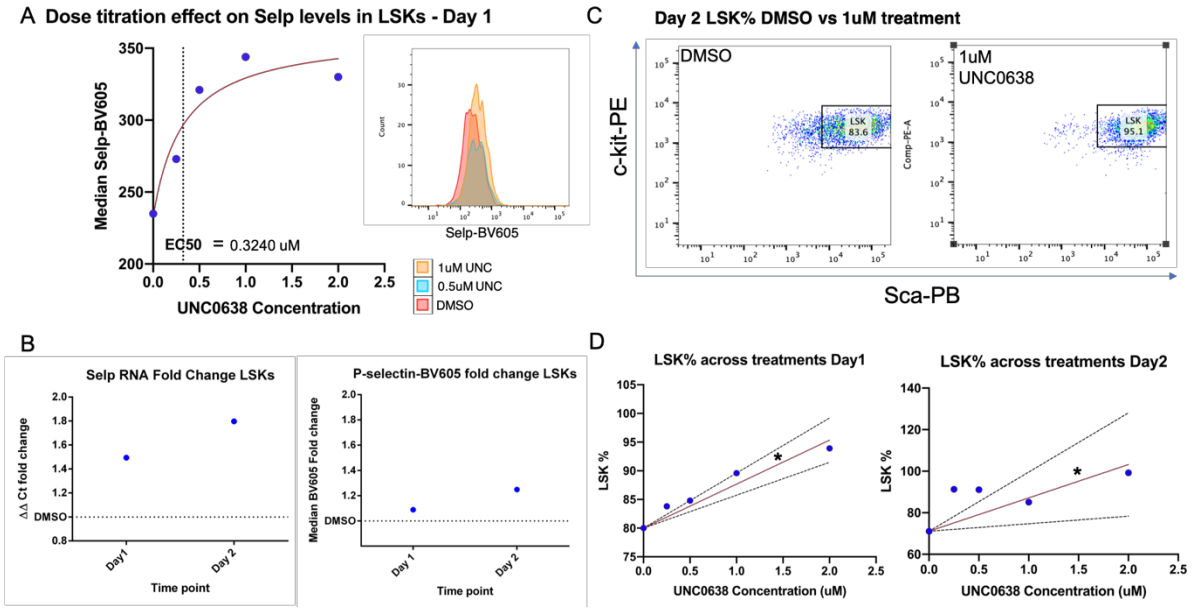

Figure 4: (A) Dose titration of UNC0638 on young LSKs plotted as median Selp-BV605 signal against inhibitor concentration; point 0.0 uM on the *x* axis corresponds to DMSO. Corresponding Selp-BV605 histogram overlay of DMSO, 0.5uM and 1.0uM UNC0638 (B) Selp RNA and protein fold-change under 1uM treatment on Day 1 and 2. (C) The LSK population on the second Day after sorting in cells 1uM UNC0638 treated cells vs DMSO control. (D) There appears to be a linear relationship between drug dosage and LSK% across 1- and 2-day exposure times. Again, 0.0 uM corresponds to DMSO control.

Table 1: UNC0638 dose titration effects on LSK%, LT-HSC% and Median Selp-BV-605 in young mouse LSK cells

Treatment	**Rep 1**						**Rep 2**					
	Day 1			**Day 2**			**Day 1**			**Day 2**		
	LSK%	LT-HSC%	Median Selp-BV605	LSK%	LT-HSC%	Median Selp-BV605	LSK%	LT-HSC%	Median Selp-BV605	LSK%	LT-HSC%	Median Selp-BV605
DMSO	80	8.21	235	71.1	11	449	97.7	9.86	471	83.6	5.12	277
0.25 uM	83.8	5.23	273	91.3	11.2	510						
0.5 uM	84.8	7.21	321	91.1	13.5	449						
1.0 uM	89.6	11.5	344	85.1	15.3	436	97.8	12.4	513	95.7	4.29	346
2.0 uM	93.9	14	330	99.2	34.8	618						

Morphology changes in treated cells

An additional observation made during FACS analysis was related to the change in morphology of both C2C12s and LSK cells upon treatment with the inhibitor. Compared to DMSO (and untreated controls), it was seen that the side scatter increased in almost all cases where the inhibitor had been used. In addition, the forward scatter was decreased, indicating smaller cells. Since side scatter is associated with cell granularity and internal complexity [26], there could be any number of changes occurring that could account for this observation.

Figure 5A shows the effects seen on SSC-A and FSC-A of 1uM UNC0638 versus DMSO in C2C12 cells. Here the dot plot is enough to see the clear shift and stark increase in side scatter. Figure 5B, shows the same data for LSK cells. However, here the shift is far more subtle and can be better visualised in the accompanying histogram wherein the SSC-A in DMSO is tinted and is observably lower than that in the treated cells.

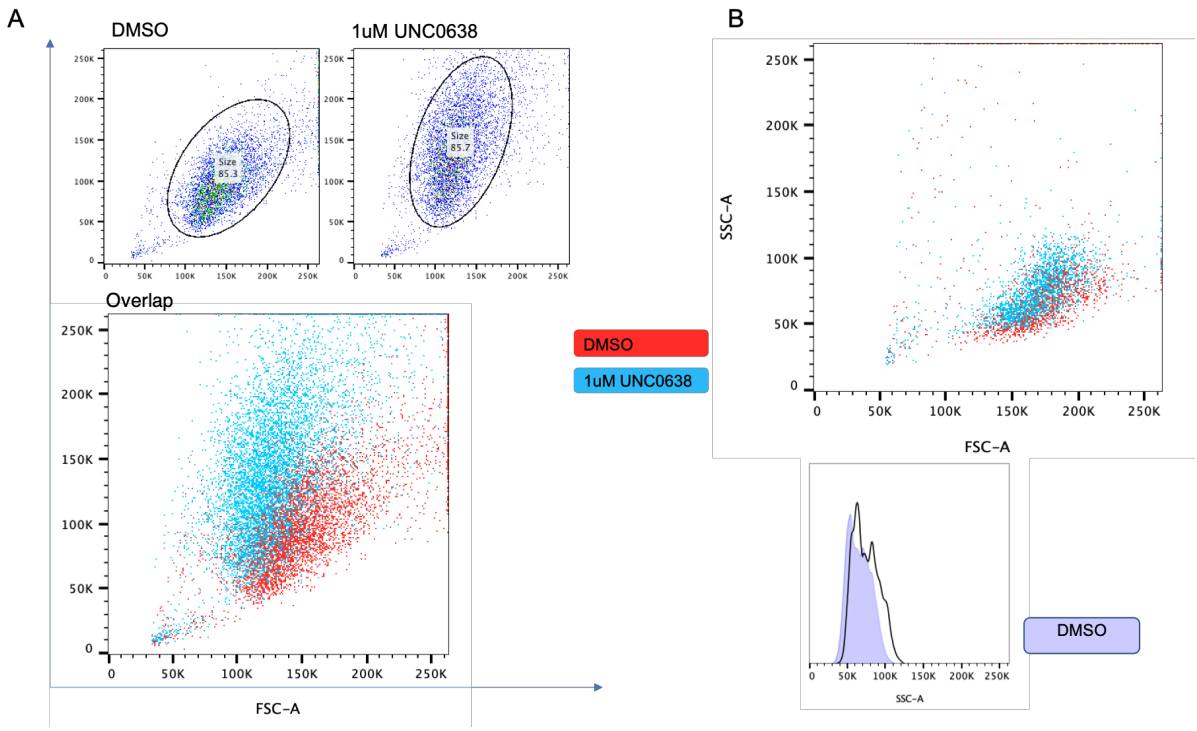

Figure 5: (A) C2C12 side scatter (SSC-A) and forward scatter forward scatter (FSC-A) plot for 1uM UNC0638 treatment (blue) compared to DMSO control (red). (B) SSC-A, FSC-A FACS plot of young LSK cells in 1uM UNC0638 versus DMSO control along with corresponding SSC-a histogram comparison.

FUNCTIONAL STUDIES OF P-SELECTIN^{HIGH} AND P-SELECTIN^{LOW} HSCS FROM OLD MICE

No significant differences in colony forming potential between P-selectin^{high} and P-selectin^{low} LT-HSCs

In order to determine whether P-selectin itself has functional effects on the HSCs where it is being expressed to a higher degree, a few in-vitro functional assays were performed. Here, it was necessary to use old mice 24-27 months of age since LSK/SLAM cells of mice in this age range constitutively express higher levels of P-selectin [14, Figure S2]. By sorting the highest and lowest 30% P-selectin-PE positive signal LSK/SLAM cells separately, it was possible to observe their functionality in single cell colony forming and CFU-GM assays.

For the single cell assays, a single cell was sorted into each well and an equal number of Selp^{high} and Selp^{low} wells were set up. For the first three days after sorting, the cells were counted, and the number of cell divisions calculated for each group. This means that 2 cells were counted as 1 division, 4 as 2 divisions and so on. Throughout this time, the proliferation potential between both groups remained more or less the same with an almost equal number of divisions per day (Figure 6A). Here, data of cells from two mice were pooled. When colonies were scored after 14 days, a similar result was seen in that the colony sizes did not vary much between both groups. Figure 6B shows separate data from two mice but emphasises the fact that the colony sizes were not influenced much by whether the starting cell was Selp^{high} or Selp^{low}.

The CFU-GM assay too, showed similar results in that the number of colonies formed appeared to be unaffected by the expression of P-selectin on HSCs (Figure 6C). It could be that this protein does not play a definitive role in affecting the ability of HSCs to form granulocytes and macrophages. Thus, it would be interesting to see whether there is any difference if the Selp^{high} and Selp^{low} cells are subjected to a CFU-Megakaryocyte (Mk) assay since Selp expression has been reported to be correlated with megakaryopoiesis.

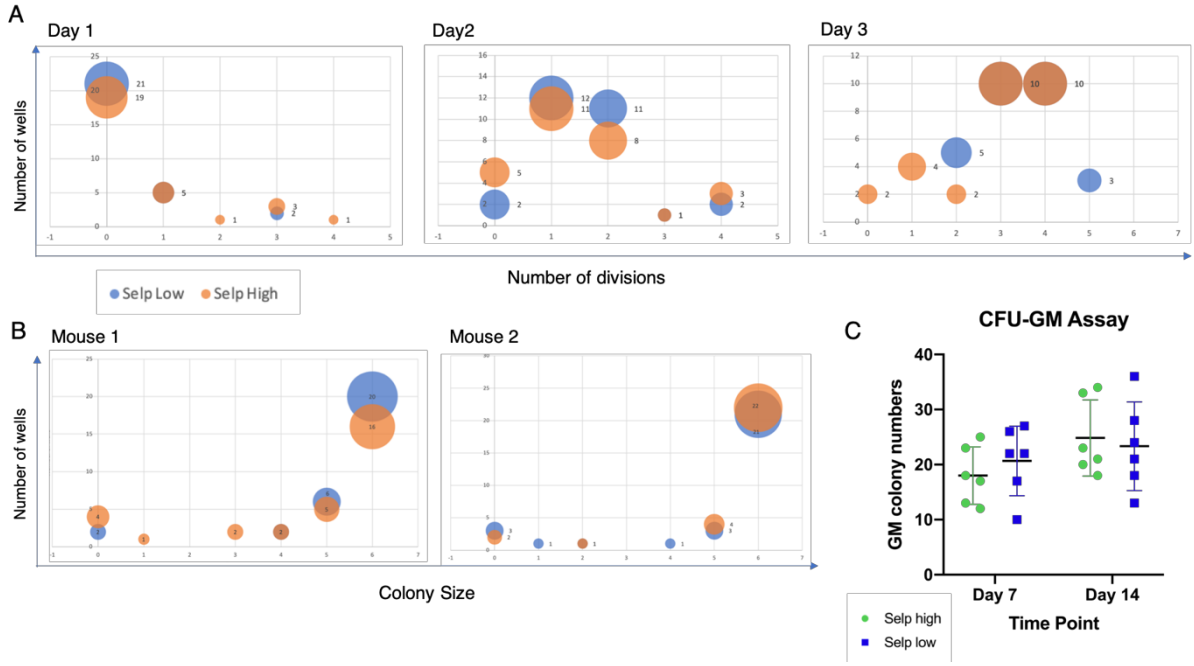

Figure 6: (A) Number of divisions undergone by single cells sorted as P-selectin^{high} and P-selectin^{low} in the first three days after sorting (B) 14-day colony size comparison between single cell P-selectin^{high} and P-selectin^{low} in two separate mice (C) CFU-GM colony numbers counted at Day 7 and 14 for 100 cells per dish P-selectin^{high} vs P-selectin^{low}

DISCUSSION

The results of experiments conducted within the scope of this research project support the primary aim which was to see if perturbations to G9a/GLP using a specific inhibitor could increase Selp expression levels. Overall, it was found that the use of the inhibitor UNC0638 increased Selp levels at the RNA and protein levels in a Selp-expressing cell line and in HSCs derived from young mice. It was also found that the self-renewal of LSKs was increased with this compound. The observations made here have been previously described in other studies [19, 21] that use this inhibitor but our focus on the age-upregulated Selp gene has led to a more detailed understanding of the effects of G9a/GLP inhibition and associated H3K9me2 levels in this context.

First, there is evidence that the effect of the inhibitor on the C2C12 cell line is similar to that in HSCs. The concentration after which cell viability decreases in HSCs was reportedly 1uM in HSCs [19] and here we found the IC50 in C2C12s to be around 1.3uM. One limitation with the adherent cell line is that the cell counts may be affected by the efficiency of the enzymatic detachment and may not have

reflected the increasing cell number reported in concentration up to 1uM because of this. However, this effect is minor, and the viability experiments were largely consistent. Although a suspension cell-line could have been investigated, very little information is available for their Selp expression and most of them tend to be cancer cell lines. It was decided that a cancer cell line may already be epigenetically perturbed and therefore not ideal for this kind of investigation.

The primary focus of this project was to observe the effect of a specific G9a/GLP inhibitor on Selp expression. In this regard, it was found that Selp RNA expression is significantly upregulated when C2C12s are subjected to UNC0638. In fact, there was some evidence of increased Selp RNA expression even in 32D (myeloid) cell lines that normally have very low expression levels of the gene (Table S1), but the use of this cell line was not pursued due to high Ct values. The average 1.8-fold change in C2C12 cells was close to the 2-fold change reported when the drug was used on HSCs [19]. Although there seemed to be no dose-dependency for RNA expression changes, it appeared that protein levels increased more significantly at higher concentrations where more cells were dying. Since this high concentration is toxic, high P-selectin expression could potentially also be explained by an inflammatory or stress response type of mechanism that may, or may not be a direct consequence of G9a/GLP inhibition. It would be beneficial to obtain more protein-level replicates to better assess these effects.

The initial 3-day treatments provided enough evidence to prove that UNC0638 does cause an increase in RNA and protein levels of Selp in C2C12s. The use of a range of doses also provided insight into the range that could then be used on primary cells. However, an earlier time point is preferred when treating HSCs to prevent extensive differentiation. Thus, 1-, 2- and 3-day time points were tested. It was clear from this data that on the first day after treatment, Selp RNA levels were already significantly increased and while the fold-change remained the same, the actual levels decreased by day 3. Since the qPCR data for Day 2 was not of good quality, and there were not enough replicates conducted, it was unclear as to whether the Selp levels peaked at Day 2 or were already declining after Day 1. However, FACS analysis suggested that the protein levels peaked at Day 2. Supporting this data was the H3K9me2 intracellular FACS showing that the effect of the inhibitor begins to wear off by Day 3 with the cell reconstituting the decreased H3K9me2 levels by this time point. Since more qPCR replicates were conducted than FACS, a clear pattern or significance cannot yet be determined for the protein level. Yet, these results are suggestive of a link between the H3K9me2 levels and the Selp RNA and protein expression levels. Further, it showed that the effect of the inhibitor was quantifiable across time-points and indicating that it should be replicable in HSCs, within a 1- to 2-day timeframe.

In HSCs (young mouse LSK cells), similar results were obtained as with C2C12s in that the protein level dose titration showed a dose-dependent increase in membrane-localised P-selectin. In fact, in this case the dose-response curve was akin to a stimulatory response seen when a drug has a stimulatory effect on a protein. Again, it is not clear whether this stimulatory response is occurring as a direct cause of G9a/GLP inhibition or as a stress response. Further, the fold change seen at the RNA level was more than that at the protein level. However, it must be noted that the protein level measurement is only capturing the P-selectin expressed on the surface, and cannot account for intracellular accumulation. However, changes seen in morphology of treated versus control cells in HSCs and C2C12s show consistency in what could be a stress response, accumulation of P-selectin within the cell or even nuclear chromatin level changes. The increased cell granularity as observed through increased side scatter could be the result of any of these but also has been associated with senescence [7].

Another interesting phenotype exhibited by the UNC0638 treated LSK cells, was the increased maintenance of LSK% (including LT-HSCs) which was a confirmation of effects described previously

[19, 21]. While these studies reported no loss in functionality of the expanded LSKs upon transplantation, we did not check the functionality of these cells in this project. However, we would have hypothesized that due to increasing Selp levels accompanying the self-renewal phenotype, the treated cells would lose some function. This is based on the fact that the meta-data analysis showed Selp is almost always upregulated with age while transplants carried out with old mouse HSCs have consistently been found to have less reconstitution potential [8]. Thus, it would have been assumed that most transplanted aged HSCs were higher in Selp expression than their younger counterparts and that treated cells with higher Selp would also perform worse. The absence of a loss of function in UNC0638 treated LSK cells is thus, potentially attributable to the reversal of the inhibitor effects as seen in the reconstitution of the H3K9me2 levels by Day 3 in our experiments.

Still, this does not necessarily explain the lack of a differential phenotype seen in our in-vitro functional assays of old mouse P-selectin^{high} or P-selectin^{low} cells. It was expected that P-selectin^{high} cells would have less colony forming potential [11]. One possibility could be that a CFU-MK experiment would reveal a clearer difference between the two populations considering that P-selectin is a megakaryocyte protein. If so, the megakaryocytic skew with age [13] could be partially explained. However, this lack of phenotype led to a more in-depth hypothesis that could explain not only our findings, but other aspects of the known HSC ageing phenotypes.

On its own, our data points to early induction of changes to Selp expression after exposure to the G9a/GLP inhibitor. Here we saw an expression change at RNA and protein levels in C2C12s and young mouse LSK cells. However, from this data alone, it could not be concluded whether these changes in Selp RNA and protein expression are a direct influence of the inhibition of G9a/GLP or another "side effect". It was speculated that some inflammatory response could be taking place in treated cells and that the morphology (granulation increase) and Selp increase are a repercussion of this. A plausible explanation was found in the work of Takahashi et. al., 2012 [18] who claim that age-associated G9a/GLP degradation in response to DNA damage induces an increase in particular inflammatory cytokines of the senescence associated secretory phenotype (SASP). It could be that the use of the inhibitor represents loss of G9a/GLP as seen with their degradation during senescence, indirectly increasing Selp expression as an artefact of senescence signalling. Since it has also been reported that HSCs of the B6 strain do not undergo senescence [6], this could also explain why our P-selectin^{high} cells from old B6 mice do not lose their ability to divide. Taking our data and literature into account, it would seem that increased Selp expression in itself is not deterministic of potential to grow and divide but is perhaps one part of a senescence-associated phenotype that may be influenced by several upstream factors. Since P-selectin interacts with the extrinsic signals and is modulated by epigenetic enzymes, it could be that in these mice the P-selectin^{high} represents a senescence-like phenotype that is still reversible when culture conditions, growth factors and the niche are conducive to growth and replication.

Although it is counterintuitive to prescribe a state of permanent replicative arrest (senescence) to HSCs, a replicative senescence modelling study [7] concludes that "replicative senescence is compatible with lifelong haematopoiesis" and explains the increased self-renewal phenotype seen with age. Thus, this and the work of Takahashi et. al. [18] opens up the possibility that loss of G9a/GLP affects Selp indirectly through an inflammatory response that can also be implicated in ageing, inflammaging and senescence. In order to follow up on this hypothesis, it could be beneficial to check whether the IL-6 and IL-8 SASP-related cytokines become increased in the medium of our experimental set up. H3K9 methylation changes are reported at the promoter of these genes [18], linked to the loss of G9a/GLP function upon induction of senescence. A ChIp experiment to determine similar changes at the Selp gene locus upon treatment with UNC0638 would be one way to check whether there is any direct

influence of G9a/GLP on Selp. One potential challenge with this is the nature of the spread of H3K9me2 marks generally makes peak-calling difficult data may often be too noisy to be conclusive. However, it may also be interesting to simply apply these SASP cytokines to the cells and see if that alone is enough to drive the increase in Selp expression as we have seen in our experiments.

Further evidence to support the idea that use of this inhibitor is potentially a reflection of senescence is found in the work of Coppé et. al. 2010 [23]. Here, an upregulation of P-selectin was reported upon induction of senescence in mouse fibroblasts as part of the SASP. Interestingly, the use of a senolytic ABT263 also rejuvenated HSCs in mice [24]. Since it was reported that $Selp^{-/-}$ HSCs are better at reconstituting blood [11] it could be that the elimination of cells expressing Selp to a high degree is tantamount to eliminating senescent cells. Thus, one potential future experiment could be to first test whether the Selp-expressing cells also express other senescence markers such as P16 or if they stain positively for β-galactosidase, and then treat mice with a senolytic to check if there is an effect on Selp expressing cells too.

Overall, the experiments carried out in this project opened up several insights into what potentially underlies the age-associated increases in Selp expression. Here we conclude that G9a/GLP and their methyltransferase activities at the loci of genes related to inflammatory signals may be playing a role in regulation of Selp. However, it is clear that the influence of these epigenetic modifiers is only a part of the story and indeed, other enzymes such as SUV39h1 should also be investigated (partially investigated Table S2), along with other members of the PRC2 complex. Additionally, the effectWe also suggest that further experiments to determine Selp's potential association with replicative senescence or inflammaging in the HSC compartment could hold some promise. In this regard, the use of alternative mouse strains such as CBA, B2 and BALB [6] may provide different insights.

Finally, it is worth trying to approach the P-selectin protein from a translational perspective with the idea to quantify circulating levels of the protein and correlate them with those in the bone marrow. If a baseline can be established, then perhaps "normal" values can be quantified, and attempts can be made to predict or cure age-related diseases. In 2004, Kappelmeyer et. al. [25] reviewed the potential of P-selectin as a disease marker showing that increased P-selectin expression has been linked to several diseases already. Thus, understanding its regulation with further experiments could be of great value.

BIBLIOGRAPHY

1. Zhang, Y. *et al.* (2018) 'Hematopoietic Hierarchy – An Updated Roadmap', *Trends in Cell Biology*. Elsevier Ltd, 28(12), pp. 976–986. doi: 10.1016/j.tcb.2018.06.001.
2. Sun, D. *et al.* (2014) 'Epigenomic profiling of young and aged HSCs reveals concerted changes during aging that reinforce self-renewal', *Cell Stem Cell*, 14(5), pp. 673–688. doi: 10.1016/j.stem.2014.03.002.
3. Krauss, S. R. and de Haan, G. (2016) 'Epigenetic perturbations in aging stem cells', *Mammalian Genome*, 27(7–8), pp. 396–406. doi: 10.1007/s00335-016-9645-8.
4. Chambers, S. M. *et al.* (2007) 'Aging hematopoietic stem cells decline in function and exhibit epigenetic dysregulation', *PLoS Biology*, 5(8), pp. 1750–1762. doi: 10.1371/journal.pbio.0050201.
5. Geiger, H., Denkinger, M. and Schirmbeck, R. (2014) 'Hematopoietic stem cell aging', *Current Opinion in Immunology*. Elsevier Ltd, 29(1), pp. 86–92. doi: 10.1016/j.coi.2014.05.002.
6. Chen, J. (2004) 'Senescence and functional failure in hematopoietic stem cells', *Experimental Hematology*, 32(11), pp. 1025–1032. doi: 10.1016/j.exphem.2004.08.001.
7. Marciniak-Czochra, A., Stiehl, T. and Wagner, W. (2009) 'Modeling of replicative senescence in hematopoietic development.', *Aging*, 1(8), pp. 723–732.
8. De Haan, G. and Lazare, S. S. (2018) 'Aging of hematopoietic stem cells', *Blood*, 131(5), pp. 479–487. doi: 10.1182/blood-2017-06-746412.
9. López-Otín, C. *et al.* (2013) 'The hallmarks of aging.', *Cell*, 153(6), pp. 1194–217. doi: 10.1016/j.cell.2013.05.039.
10. Zimmerman, G. A. (2002) 'Two by two: The pairings of P-selectin and P-selectin glycoprotein ligand 1', *Proceedings of the National Academy of Sciences*, 98(18), pp. 10023–10024. doi: 10.1073/pnas.191367898.
11. Sullivan, C. *et al.* (2011) 'Functional ramifications for the loss of p-selectin expression on hematopoietic and leukemic stem cells', *PLoS ONE*, 6(10), pp. 1–10. doi: 10.1371/journal.pone.0026246.
12. Haas, S. *et al.* (2015) 'Inflammation-Induced Emergency Megakaryopoiesis Driven by Hematopoietic Stem Cell-like Megakaryocyte Progenitors', *Cell Stem Cell*, 17(4), pp. 422–434. doi: 10.1016/j.stem.2015.07.007.
13. Choudry, F. A. and Frontini, M. (2016) 'Epigenetic Control of Haematopoietic Stem Cell Aging and Its Clinical Implications', *Stem Cells International*, 2016. doi: 10.1155/2016/5797521.
14. Djeghloul, D. *et al.* (2016) 'Age-associated decrease of the histone methyltransferase SUV39H1 in HSC perturbs heterochromatin and B lymphoid differentiation', *Stem Cell Reports*, 6(6), pp. 970–984. doi: 10.1016/j.stemcr.2016.05.007.
15. Mozzetta, C. *et al.* (2014) 'The Histone H3 Lysine 9 Methyltransferases G9a and GLP Regulate Polycomb Repressive Complex 2-Mediated Gene Silencing', *Molecular Cell*, 53(2), pp. 277–289. doi: 10.1016/j.molcel.2013.12.005.
16. Shinkai, Y. and Tachibana, M. (2011) 'H3K9 methyltransferase G9a and the related molecule GLP', *Genes and Development*, 25(8), pp. 781–788. doi: 10.1101/gad.2027411.
17. rani Shankar, S. *et al.* (2013) 'G9a Structure and Activity G9a, a multipotent regulator of gene expression', *Review Epigenetics*, 8(1), pp. 16–22. doi: 10.4161/epi.23331.

18. Takahashi, A. *et al.* (2012) 'DNA damage signaling triggers degradation of histone methyltransferases through APC/C Cdh1 in senescent cells', *Molecular Cell*. Elsevier Inc., 45(1), pp. 123–131. doi: 10.1016/j.molcel.2011.10.018.
19. Ugarte, F. *et al.* (2015) 'Progressive Chromatin Condensation and H3K9 Methylation Regulate the Differentiation of Embryonic and Hematopoietic Stem Cells', *Stem Cell Reports*, 4(1), pp. 155–169. doi: 10.1016/j.stemcr.2014.11.002.
20. Vedadi, M. *et al.* (2012) 'A chemical probe selectively inhibits G9a and GLP methyltransferase and genanylgeranyltransferase I with antitumor activity against breast cancer in vivo.', *Nature chemical biology*, 7(8), pp. 566–574. doi: 10.1038/nchembio.599.A.
21. Chen, X. *et al.* (2012) 'G9a/GLP-dependent histone H3K9me2 patterning during human hematopoietic stem cell lineage commitment', *Genes and Development*, 26(22), pp. 2499–2511. doi: 10.1101/gad.200329.112.
22. Li, S. *et al.* (2018) 'JMJD1B Demethylates H4R3me2s and H3K9me2 to Facilitate Gene Expression for Development of Hematopoietic Stem and Progenitor Cells', *Cell Reports*. ElsevierCompany., 23(2), pp. 389–403. doi: 10.1016/j.celrep.2018.03.051.
23. Coppé, J. P. *et al.* (2010) 'A human-like senescence-associated secretory phenotype is conserved in mouse cells dependent on physiological oxygen', *PLoS ONE*, 5(2). doi: 10.1371/journal.pone.0009188.
24. Luo, Y. *et al.* (2015) 'Clearance of senescent cells by ABT263 rejuvenates aged hematopoietic stem cells in mice', *Nature Medicine*. Nature Publishing Group, 22(1), pp. 78–83. doi: 10.1038/nm.4010.
25. Kappelmayer, J. *et al.* (2004) 'The emerging value of P-selection as a disease marker', *Clinical Chemistry and Laboratory Medicine*, 42(5), pp. 475–486. doi: 10.1515/CCLM.2004.082.
26. Taylor, I 'Forward scatter vs side scatter', FlowJo, https://www.flowjo.com/learn/flowjo-university/flowjo/getting-started-with-flowjo/58
27. FlowJo v10 Documentation, http://docs.flowjo.com/d2/experiment-based-platforms/population-comparison/

SUPPLEMENTAL INFORMATION

Figure S1: FACS plots for LT-HSCs in DMSO vs. 1uM UNC0638 treatment conditions

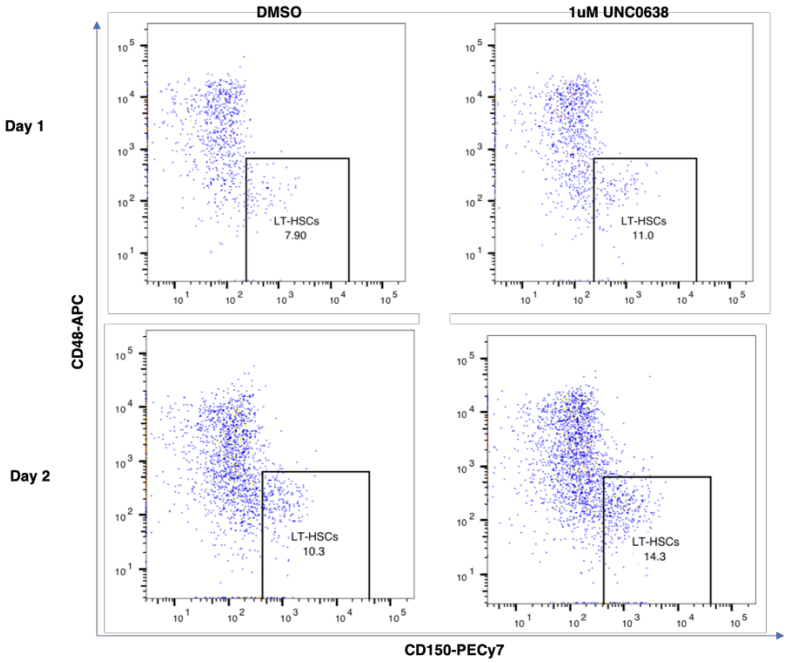

Figure S2: Selp RNA expression in primary cells from old and young mice

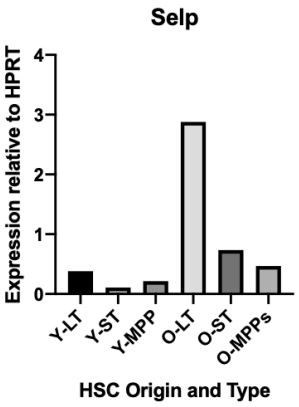

Table S1: Treatment of 32D cells with UNC0638 Selp RNA Expression

Treatment	RNA Expression	
	Ct Value	**ΔΔCt Fold change**
DMSO (Plate 1)	26.61	
DMSO (Plate 2)	26.74	
0.125 uM	26.07	1.1
0.25 uM	25.70	2.1
0.5 uM	25.65	2.3
1.0 uM	25.69	1.9
2.0 uM	27.16	0.9

Table S2: FACS data for SUV39h1 inhibitor Chaetocin treatment of C2C12 cells

Treatment		
	Selp+%	**Median Selp-BV605**
DMSO	2.43	244
0.5nM	1.91	241
1nM	1.55	248
2.0nM	0.68	229
4.0nM	0.52	224
8.0 nM	0.81	241